

Hippocampal Afterdischarges after GABA_B-Receptor Blockade in the Freely Moving Rat

L. Stan Leung, Kevin J. Canning, and Bixia Shen

Departments of Physiology-Pharmacology and Clinical Neurological Sciences, University of Western Ontario, London, Ontario, Canada

Summary: *Purpose:* To determine whether hippocampal afterdischarges (ADs) and excitability changes were induced by γ -aminobutyric acid (GABA)_B-receptor blockade in adult, freely moving rats.

Methods: A specific GABA_B-receptor antagonist CGP35348, CGP55845A, or CGP56999A was injected intracerebroventricularly (i.c.v.), and EEGs and behaviors of rats were analyzed.

Results: CGP35348 (56–110 μ g, i.c.v.) induced afterdischarges (ADs) ~60% of the time, starting at the hippocampus or neocortex. Neocortical-onset ADs began with sporadic discharges and were <3 mV. Hippocampal-onset ADs were bilateral, >5 mV, and spread to the entorhinal cortex and amygdala, often ending in a rebound AD and accompanied with stereotypic jumping, forelimb clonus, and wet-dog shakes. The CGP35348-induced hippocampal AD had an onset frequency (5–9 Hz) that was higher than the electrically evoked AD (2–4 Hz). CGP35348 i.c.v. also increased the mean starting frequency of an electrically

evoked hippocampal AD from 3.6 Hz to 5.3 Hz. Hippocampal gamma activity (25–80 Hz) increased up to twofold for 30 min after a hippocampal but not a neocortical AD. A single dose of CGP35348 induced repeated ADs of increasing duration. Paired-pulse inhibition of the evoked potentials in CA1, at interpulse interval of <100 ms, was decreased after but not before a hippocampal AD. CGP56999A (i.c.v.) gave results similar to those with CGP35348, whereas CGP55845A (i.c.v.) rarely induced ADs.

Conclusions: GABA_B-receptor blockade increases seizure susceptibility by reducing AD threshold and increasing the frequency and spread of a hippocampal AD. Hippocampal excitability (based on paired-pulse test) and gamma activity increased after but not before a hippocampal AD. **Key Words:** CGP35348—Gamma waves—Theta rhythm—Kindling—Paired-pulse depression.

γ -Aminobutyric acid (GABA) is the main inhibitory neurotransmitter in the cerebral cortex, and it mediates inhibition through GABA_A and GABA_B receptors. GABA_A-receptor functions are relatively well understood. Suppression of GABA_A-receptor function induces seizures (1,2), whereas GABA_A-receptor agonists are effective anticonvulsants. In contrast, the participation of GABA_B receptors in partial (focal) seizure generation is not well established.

Despite their effectiveness against generalized absence seizures (3,4), GABA_B-receptor antagonists were found to induce convulsive, presumably partial seizures in rats (5–7). GABA_B-receptor antagonists also induced epileptiform activity in vitro (8,9), and one type of GABA_B-receptor polymorphism has been associated with tempo-

ral lobe epilepsy in humans (10). The GABA_B-receptor R1 knockout mice was reported to manifest spontaneous generalized seizures (11,12), but the origin of the seizures was not clear. In studies that induced seizures by GABA_B-receptor antagonists, EEG was not used in seizure detection except in one study (5).

We are interested in the conditions in which GABA_B-receptor blockade may lead to seizures. Although the functions of several types of GABA_B receptors (4) may be different, the cumulative evidence suggests that overall GABA_B-receptor blockade increases seizure susceptibility. In particular, we suggest that the hippocampus, which has a low seizure threshold, will be destabilized by GABA_B-receptor blockade. Thus we hypothesize that partial (focal) seizures originate from the hippocampus after intracerebroventricular (i.c.v.) administration of a GABA_B-receptor antagonist in rats. Three different GABA_B-receptor antagonists, CGP35348, CGP55845A, and CGP56999A, were used to test this hypothesis. EEGs and hippocampal evoked potentials were used to study the changes in hippocampus and neocortex before, during, and after a seizure.

Accepted October 11, 2004.

Address correspondence and reprint requests to Dr. L.S. Leung at Department of Clinical Neurological Sciences, 399 Windermere Rd., London Health Science Centre—University Campus, University of Western Ontario, London, Ontario, Canada N6A 5A5. E-mail: sleung@uwo.ca

Present address of Dr. Kevin J. Canning: GlaxoSmithKline, Inc. (Canada), Basic Research/Genetics R & D, 7333 Mississauga Rd. N, Mississauga, ON L5N6L4, Canada.

METHODS

Animals, surgical, and injection procedures

Male Long-Evans rats (250–400 g) 2 months old or older were operated on while under sodium pentobarbital anesthesia (65 mg/kg, i.p.). The surgically exposed dorsal skull surface was positioned horizontally in a stereotaxic apparatus. With bregma as a reference, holes were drilled at various sites for placement of recording electrodes and cannulae (13). Deep and shallow electrodes were placed at P4.5, L3.0, 3.5, and 2.5 mm ventral (V) to skull surface, targeted at stratum radiatum of dorsal hippocampal CA1 and deep layers (5 or 6) of the parietal neocortex, respectively. In addition to local EEG activity, the neocortical electrode recorded dorsal hippocampal activity by volume conduction. In some rats, electrodes also were placed in the medial entorhinal cortex (P8.0, L4.4, and V7.6) and the basolateral amygdala (P2.8, L5.0, and V8.5). Electrodes were 125- μ m stainless steel wires coated with Teflon insulation except at the cut tip. Twenty-three-gauge stainless steel tubing, serving as guide cannulae for lateral ventricle injections, was implanted at P0.8, L1.4. All cannulae and electrodes were permanently fixed to jeweler screws in the skull with acrylic dental cement. Animals were allowed to recover for 1 week.

Various doses of GABA_B-receptor antagonists were injected i.c.v. The GABA_B-receptor antagonists, kindly provided by W. Froestl of Novartis, were *P*-(3-aminopropyl)-*P*-diethoxymethyl-phosphinic acid (CGP35348) (14,15), 3-[1-(*S*)-(3,4-dichloro-phenyl-ethyl)amino-2-(*S*)-hydroxy-propyl-benzyl-phosphinic acid (CGP55845A) (16), and 3-[1(*R*)-[(3-cyclohexylmethyl-hydroxyphosphinoyl)-2(*S*)-hydroxypropyl-amino]-ethyl]benzoic acid lithium salt (CGP56999A) (8). Each drug was dissolved in artificial cerebrospinal fluid (aCSF, in mM: NaCl, 124; KCl, 5; NaH₂PO₄·H₂O, 1.25; MgSO₄·7H₂O, 2; CaCl₂·6H₂O, 2; NaHCO₃, 26; and glucose, 10). A 30-gauge needle attached to PE-10 tubing and connected to a Hamilton microsyringe was filled with mineral oil, and the drug or vehicle (aCSF) was drawn into the needle tip. The needle was designed to protrude 1–2 mm beyond the ventral tip of the guide cannula, to reach the lateral ventricle at a depth of V \sim 3.4 mm. Injection was performed over approximately a 30-s period, and the needle was extracted 1 min after injection. A dose of CGP35348 (MW, 232.42) of 28, 56, 110, 220, or 330 μ g dissolved in 1.5–3 μ l of aCSF, was injected into one ventricle. Assuming a 1.5-ml dilution volume in the CSF, the estimated i.c.v. concentrations were \sim 80, 160, 320, 630, or 950 μ M, respectively, for the doses of CGP35348 listed earlier. Similarly, 0.21, 0.84, 3.36, 6.6, and 20 μ g of CGP55845A (MW, 438.72) was injected in 1.5–3 μ l of aCSF to give estimated i.c.v. concentrations of 0.32, 1.28, 5.1, 10, and 30 μ M. CGP56999A (MW, 425.03) was given in a 1.5- μ l solution of aCSF, containing 0.48 and 0.96 μ g, to

give estimated i.c.v. concentrations of 0.75 and 1.5 μ M. In the hippocampal slice in vitro, 160 μ M CGP35348 blocked postsynaptic (15) but not presynaptic GABA_B receptors (14), whereas \geq 1.28 μ M CGP55845A (and CGP56999A) blocked both presynaptic and postsynaptic GABA_B receptors in hippocampal CA1 (16).

An afterdischarge (AD) was operationally defined as paroxysmal activity of >5-s duration and with peak-to-peak amplitude at least twice that of the baseline background EEG. Most rats were given more than one dose of a GABA_B-receptor antagonist. If an AD was not induced for a given dose, a higher dose was used in a subsequent experiment, \geq 4 days later. If an AD was induced, a lower dose was used until no AD was induced. For each dose except the highest used for each drug, there were always naive rats that received that dose as the first injection. Unless otherwise noted, data from rats that had more than three previous injections or more than two experiments with ADs were excluded.

In some rats, a hippocampal AD was electrically evoked by a high-frequency stimulus train applied at a CA1 stratum radiatum electrode. The train consisted of a 1-s train of 100-Hz pulse of 0.1-ms pulse duration and stimulus intensity of 100–400 μ A (17). Repeated electrically induced ADs were delivered every hour, 5 times a day, and for a total of 15 ADs in 3 days. This is called partial hippocampal kindling, because no motor convulsions were typically induced after 15 ADs evoked in the dorsal hippocampus (18). In other rats, stimulation trains (200-Hz pulses of 0.1-ms duration) near the AD threshold intensity (40–80 μ A) were delivered to CA1, 15 min after either saline or CGP35348 i.c.v. injections. Saline and CGP35348 experiments on the same rat were separated by >4 days.

Electrophysiologic and behavioral analysis

Hippocampal EEG was recorded continuously on paper by a Grass 7D polygraph, with annotation of animal behavior on the EEG paper. On occasion, animal behavior was videotaped for off-line analysis ($n = 13$). Behavioral seizures were classified according to the five stages of Racine (19). Hippocampal EEG before, during, and after an AD was sampled at 200 Hz and stored on a microcomputer. Logarithmic power spectrum (autopower) for single-channel EEG, and coherence (Fisher *z*-transform) and phase spectra of the EEGs across two channels were calculated by methods described elsewhere (20). Segments of EEG of 1,024 points (5.12 s) were used for Fast Fourier Transform, yielding resolution of 0.195 Hz, and 2.15 Hz bandwidth after smoothing. For each 5.12 s used, the spectrum had 22 degrees of freedom. Spectral analysis of the AD used the first 10.24 s during the AD onset, and spontaneous EEG (before or after AD) typically used >30.72 s of EEG.

Average evoked potentials were recorded at electrodes in the stratum radiatum and the alveus of dorsal CA1 (P3.5,

L2.7), and averages of four sweeps were used unless otherwise indicated. For paired-pulse depression (PPD) studies, paired-pulse responses of 30–100 ms interpulse interval (IPI) were recorded after stimulation of the apical dendritic afferents to CA1. The stimulus pulses (100- to 600- μ A intensity and 0.1-ms pulse duration) were given at ≥ 9 -s intervals. Stimuli were given when the rat was awake and immobile, except for times immediately around an AD, when the stimuli were given irrespective of rat behavior. Evoked responses were filtered from 0.1 Hz to 2.5 KHz and digitized at 7 KHz by using a customized program. A population spike was measured from its onset to peak, and the peak of the population excitatory postsynaptic potential (pEPSP) was measured from the baseline before the shock artifact. Paired-pulse ratio was calculated as the ratio of the response to the second pulse to that of the first pulse. Paired-pulse ratio of < 1 indicates PPD (e.g., when the population spike in response to the second pulse was less than that in response to the first pulse).

The effect of the GABA_B-receptor antagonist to block the effect of baclofen was studied in rats anesthetized with urethane (1.5 g/kg, i.p.). Hippocampal evoked potentials were recorded and averaged at 16 channels of a silicon electrode placed in dorsal CA1 (21). The multichannel electrode recorded from different depths in CA1 at 50- μ m intervals. Current source density (CSD) was calculated by a second-order spatial differencing of the potentials at one time instant (21). \pm Baclofen (10 nmole, i.c.v.) induced a clear effect on the paired-pulse evoked potentials in CA1, at IPI of 50 ms, after stimulation of CA3. In other rats, injection of CGP35348 or CGP55845 was made ~ 30 min before baclofen, and the response after baclofen was compared with the baseline before any drug. The rising slope of the excitatory current sink at CA1 stratum radiatum, after CSD analysis, was determined for a 1-ms interval near onset, after the first (E1) or the second pulse (E2).

Group measures are presented as mean \pm standard error of the mean (SEM). Nonparametric statistics were performed, by using the Wilcoxon test, and $p < 0.05$ was considered statistically significant.

Histology

After experimentation, animals were killed by transcardial perfusion of saline followed by 10% formalin under deep urethane anesthesia. The brains were removed and cut into 40- μ m-thick coronal sections and stained with thionin. The recording electrodes, stimulation electrodes, and cannula locations were verified in the histologic sections.

RESULTS

Hippocampal afterdischarges induced by i.c.v. CGP 35348

Electrical seizures or ADs were observed after CGP35348 (56 or 110 μ g, i.c.v.) injection in $\sim 60\%$ of the rats (Table 1). Evoked response and single-unit recordings in the hippocampus indicated that the action of i.c.v. CGP35348 peaked at ~ 30 min after injection and returned to baseline at > 70 min (data not shown). Thus only the number of ADs in the first hour was analyzed (see Table 1). Increasing CGP35348 dose increased the reliability of eliciting ADs, and the ADs were associated with more severe seizure stages. Increasing CGP35348 dose decreased the mean AD onset time, but not significantly (see Table 1). Two main types of ADs were distinguished, those of hippocampal onset and those of neocortical onset, each constituting $\sim 50\%$ of the total number of ADs studied.

The hippocampal-onset AD had an abrupt high-amplitude paroxysmal activity, with the earliest onset in the hippocampus (Figs. 1A, 2A, and 3B). The primary (1°) hippocampal AD was ~ 35 -s duration, with sharp discharges recorded in CA1 and CA3c in the hilus (Fig. 1A). When recorded across the CA1 cell layer, the main discharges were positive and > 5 mV at CA1 stratum radiatum and negative dorsal to the CA1 cell layer (Fig. 2A and D). The main AD consisted of rhythmic 5- to 9-Hz discharges that were bilateral in the hippocampus (Figs. 2A and D, 3B). An entorhinal or amygdala AD was not detected before a hippocampal AD (see Fig. 1), but sometimes the ADs appeared to start simultaneously at the hippocampus, entorhinal cortex, and amygdala (not

TABLE 1. Characteristics (mean \pm SEM) of hippocampal afterdischarges (ADs) induced by i.c.v. CGP35348

Dose of CGP35348 (μ g)	56	110	220	330
Estimated concentration (μ M i.c.v.)	160	320	630	950
Number of rats	9	14	9	7
Number showing AD in 1 h	5	9	7	7
Percentage showing AD in 1 h	56%	64%	78%	100%
Latency of AD onset (min) ^a	22 \pm 5	13 \pm 3	17 \pm 4	7 \pm 3
Duration of first AD (s) ^a	26 \pm 4	34 \pm 6	55 \pm 13	55 \pm 11
Mean behavioral seizure stage ^b	0.6 \pm 0.3	1.4 \pm 0.6	1.7 \pm 0.5	4.1 \pm 0.3
Average no. ADs within 1 h	1.2 \pm 0.2	1.9 \pm 0.3	1.9 \pm 0.3	4 \pm 1.2

Except for the highest dose used, animals that had more than three injections and two or more afterdischarges (ADs) in previous injections were not included.

^aLatency and duration measures are from animals that had ADs.

^bSeizure stage according to classification of Racine (1972); pure jumping considered as stage 0.

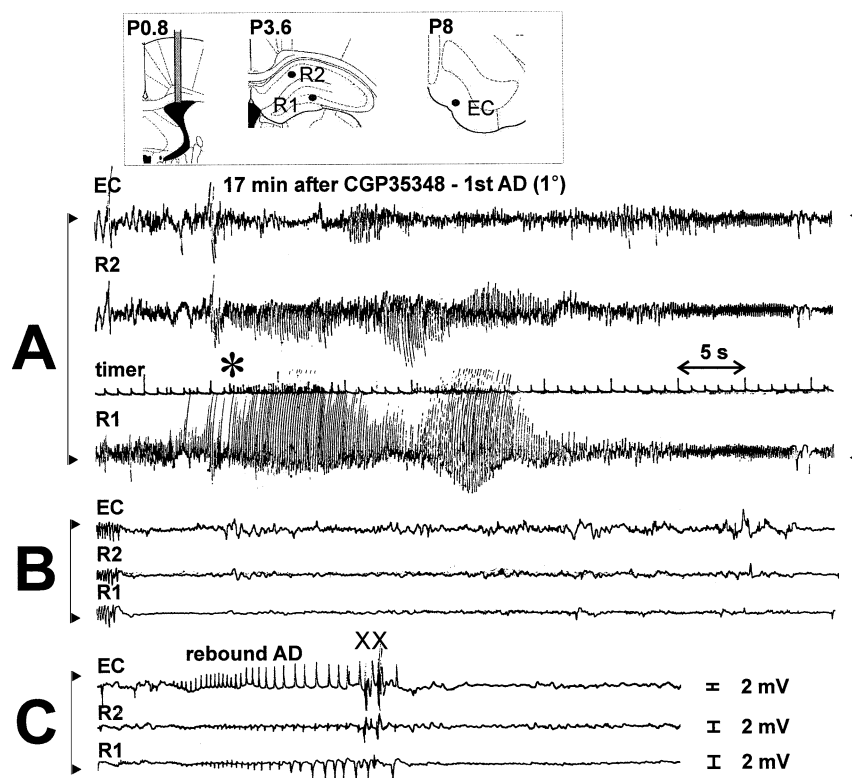


FIG. 1. Characteristic pattern of primary and rebound hippocampal afterdischarge induced by intracerebroventricular (i.c.v.) injection of CGP35348. **Inset, from left to right:** Cannula inserted into the lateral ventricle, posterior to bregma (P) 0.8 mm; hippocampal R1 (at CA3c) and R2 (at CA1 stratum radiatum) electrodes at P3.6; medial entorhinal cortex (EC) at P8; sections from atlas of Paxinos and Watson (13). **A–C:** Continuous EEG recordings at the start of an afterdischarge (AD) after injection of CGP35348 (110 μ g, i.c.v.; first injection in rat R749). EEG derived from the hippocampal electrodes R1 and R2 and medial entorhinal cortical electrode EC, shown with a timer trace. **A:** At 17 min after injection, a primary (1°) AD was observed at R1 and R2 electrodes (*) and spread later to the EC. **B:** Silent period of hippocampal EEG. **C:** Rebound AD at the hippocampus appeared slightly later than that at EC. The rat was immobile during the AD except during a wet-dog shake (X) at the end of the rebound AD. EEG is positive up.

shown). A rebound AD appeared in the hippocampus (Figs. 1C and 3B2), at >90 s after the onset of the 1° hippocampal AD, and after a period of relative EEG silence (Figs. 1B and 3B2). Rebound AD also is known as secondary AD, but to avoid confusion with the second AD induced by the same CGP35348 injection, only the term *rebound AD* is used. The animal usually remained immobile during the 1° AD, but wet-dog shakes (XX in Figs. 1C and 3B2) were frequent during the rebound AD. Postictal depression of the EEG followed the rebound AD.

In about one third of hippocampal-onset ADs, uni- and bilateral forelimb clonus (stage 3 seizure), sometimes with rearing (stage 4 seizure) or rearing and falling (stage 5), were observed during the hippocampal AD (Figs. 2A and 3B). In other cases, a rat jumped several times stereotypically during the 5- to 8-Hz hippocampal AD (Fig. 4A). A short hippocampal AD (<20 s) may be accompanied by a brief period of jumps (Fig. 4A), during and after which no motor convulsions were observed. The jumps could be provoked by sensorimotor stimuli, such as an experimenter touching the animal or just walking toward the animal's cage. Jumping of limited duration was assigned seizure stage zero. Violent and prolonged multiple jumps,

alternating with running, were usually followed by generalized seizure and tonic-clonic convulsions.

Theta-frequency activity immediately before and during the afterdischarge

A detailed pattern of EEG around a hippocampal AD is shown in Fig. 2. The onset of abnormal activity started at an arrow (\uparrow) in Fig. 2A, with the appearance of 9.8-Hz EEG activity (Figs. 2B and 5A), during apparently normal rearing in the rat. The 9.8-Hz activity was abnormal because of its sharp waveform and prolonged (>10 s) duration, but it was not considered to be part of the AD (that was operationally defined as $>2\times$ background EEG amplitude). Spectral analysis confirmed that 9.8 Hz was the mean frequency at all hippocampal electrodes (Fig. 5A). In addition, the 9.8-Hz activity was coherent between electrodes that straddled the CA1 cell layer (i.e., L1–L2 and R1–R2 electrodes) and with a phase shift of $\sim 150^\circ$. The latter phase shift was similar to that of the normal theta rhythm (not shown). The sharpness of the waves (Fig. 2B) was confirmed by the multiple theta harmonics in the power spectra (arrows in Fig. 5A), with EEG at R2 electrode showing more than three harmonics (first

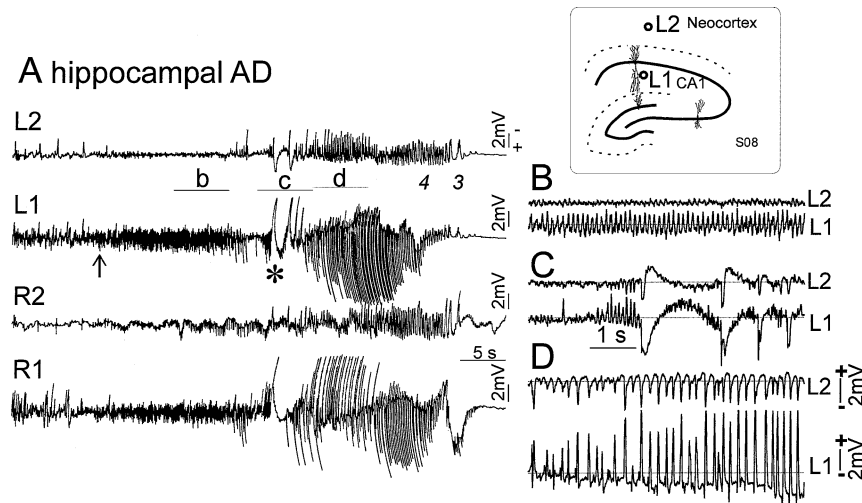


FIG. 2. Bilateral hippocampal onset afterdischarges after γ -aminobutyric acid (GABA)_B-receptor blockade started with theta-frequency discharges. GABA_B-receptor antagonist CGP35348 (220 μ g, i.c.v.) was injected on the left lateral ventricle and induced afterdischarges (ADs) for the first time in this rat (S08). **Inset on right:** Schematic with electrode location of L2 and L1 after histologic verification; R2 and R1 were located on the contralateral side at similar locations as L2 and L1, respectively. **A:** The paroxysmal event occurred 31 min after injection of CGP35348 and started with sharp, high-frequency hippocampal theta (\uparrow below L1 trace, continuing into period "b"). Period "c" indicates the start of the high-amplitude AD, which continued as bilateral discharges in the 5- to 7-Hz frequency range (period "d"). Number in italics after period "d" indicates stages 4 (rearing with bilateral forelimb clonus) and 3 (unilateral right forelimb clonus). No rebound AD was observed, but postictal depression was seen (not shown). **B–D:** Detailed patterns of the EEG at L2 and L1 during periods b, c, and d, respectively, as indicated in **A**. Polarity of EEG is negative up in **A**, and positive up in **B–D**.

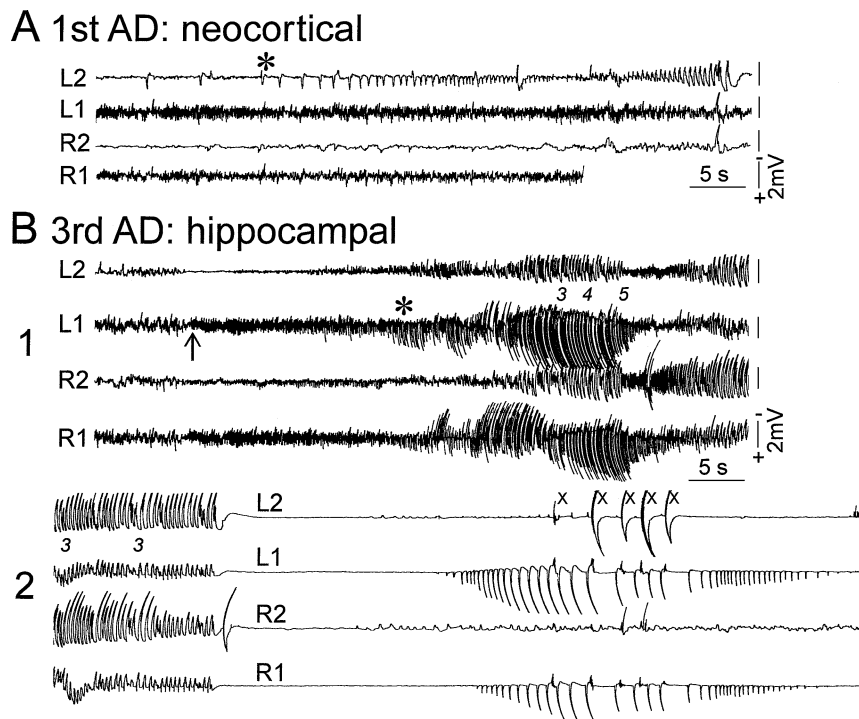


FIG. 3. γ -Aminobutyric acid (GABA)_B-receptor blockade induced both neocortical- and hippocampal-onset afterdischarges (ADs). GABA_B-receptor antagonist CGP35348 (220 μ g, i.c.v.) was injected in rat S08, the same injection as Fig. 2. **A:** Neocortical-onset AD (*) induced by CGP35348 at 16 min after injection. The AD was restricted to L2 and did not result in postictal EEG depression (not shown). **B:** Hippocampal-onset AD induced at 47 min after injection, 16 min after the last hippocampal AD shown in Fig. 2. Sharp, high-frequency theta waves (\uparrow) occurred before the start of the AD, which showed seizure stages 3, 4, and 5 (rear and fall), and rebound AD, during which wet-dog shakes (X) occurred. B2 is continuation of B1. EEG is negative up.

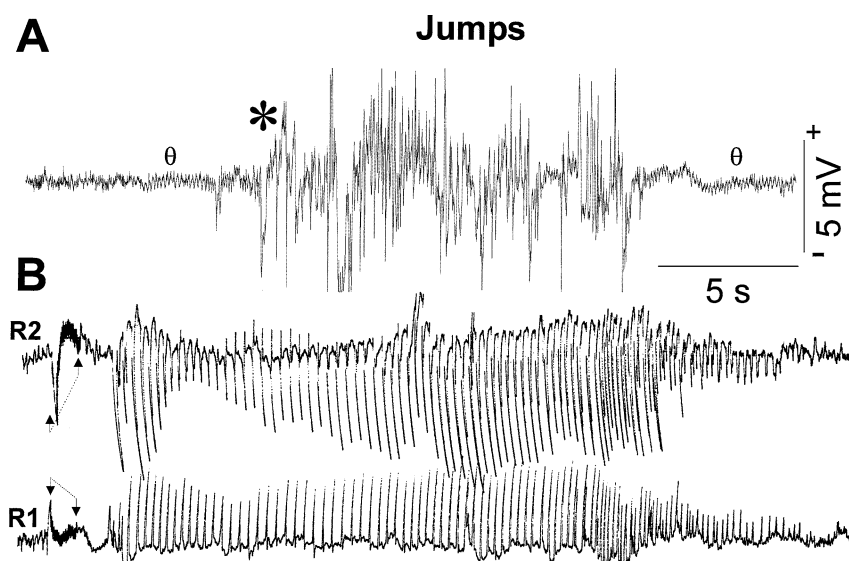


FIG. 4. Hippocampal afterdischarge (AD) frequency was higher when induced by i.c.v. CGP35348 than by electrical stimulation. **A:** AD induced by CGP35348 i.c.v. was accompanied by repeated jumps of the rat (R769); AD (onset at $*$) was recorded at stratum radiatum of CA1. The main AD frequency was 7 Hz, as assessed by power spectral analysis (not shown). Normal theta (θ) waves preceded and followed the AD. **B:** AD induced by an electrical train stimulation showed a main frequency of ~ 2 Hz. The AD was recorded at electrodes placed in the CA1 alveus (R2) and stratum radiatum (R1), and was induced by 1-s, 100-Hz, and 250- μ A stimulus pulses applied to the contralateral CA1 (between arrows linked by a dotted line). Calibration applies to both **A** and **B**; EEGs are shown positive up.

and third harmonics labeled as θ_1 and θ_3 , respectively, in Fig. 5A3).

The high-amplitude hippocampal AD also was subjected to spectral analysis. In the example shown, a frequency peak of 5.9 Hz was detected during the first 10.2 s of the AD (Fig. 5B), as expected for the rhythmic signals (Fig. 2D). Based on polygraph recordings, the early discharges (< 10 s) of the hippocampal AD induced by CGP35348 were estimated to have a frequency of 6.4 ± 0.4 Hz (mean \pm SEM; $n = 18$).

The 6.4-Hz mean frequency of the hippocampal AD induced by CGP35348 i.c.v. contrasts with the slower frequency during an AD evoked by electrical stimulation (17). The electrically induced AD started, after 2–3 s of depressed EEG, with 2- to 4-Hz ictal discharges (Fig. 4B). In 16 rats with electrically evoked ADs (no CGP35348 was given), the initial ictal discharge frequency (average over a 2-s period) was 3.6 ± 0.1 Hz ($n = 16$) for the first AD, evoked by a train stimulus intensity of 250 ± 14 μ A ($n = 16$). After partial hippocampal kindling (five hourly ADs for 3 days for a total of 15 hippocampal ADs), the initial AD frequency was 3.8 ± 0.2 Hz ($n = 16$) for AD 15, not significantly different ($p > 0.2$, paired Wilcoxon) from that of the first AD. In contrast, the AD duration increased significantly from 24 ± 2 s for the first AD to 70 ± 5 s for AD 15 ($p < 0.01$, paired Wilcoxon; $N = 16$). Thus the initial frequency of an electrically evoked AD was not dependent on the AD duration, and the AD morphology and frequency remained the same for the first 10–15 s for ADs of different durations.

In separate experiments using stimulus trains near the AD threshold intensity (Methods), CGP35348 (28–175 μ g, i.c.v.) was found to decrease the AD threshold in 10 paired experiments with seven rats. In six rats given a dose of 56 μ g, i.c.v., CGP35348, a stimulus train induced an AD duration of 42 ± 1 s ($n = 6$), significantly ($p < 0.05$, paired Wilcoxon) longer than the AD induced by the same stimulus train in the same rat after i.c.v. saline. After saline, no AD was induced in two rats, and a short AD duration of 8.6 ± 1 s ($n = 4$) was induced in the other four rats (all with < 12 -s AD duration). The initial frequency of the electrically induced AD after i.c.v. saline was 4 ± 0.2 Hz ($n = 4$), not different from the larger group of 16 rats (without i.c.v. injections) reported above. In the rats given 56 μ g i.c.v. CGP35348, the AD initial frequency was 5.3 ± 0.2 Hz ($n = 6$), significantly higher ($p < 0.05$, Wilcoxon) than that in rats without CGP35348 (3.6 ± 0.1 Hz; $n = 16$). Thus i.c.v. CGP35348 increased the initial frequency of the AD evoked by electrical stimulation.

Neocortical-onset ADs

The neocortical-onset AD was characterized by abnormal EEG spikes that occurred at low frequency ($< 1/s$) at an electrode in or near the parietal neocortex. EEG spikes could occur for minutes before an AD (AD onset marked by $*$ in Fig. 3A), and they were categorized as “EEG spikes” (and not ADs) because these abnormal events were infrequent and transient, and the EEG between the “spikes” appeared normal. In the example shown, the EEG spikes were likely generated by the neocortex, being larger at the electrode in the neocortex (L2)

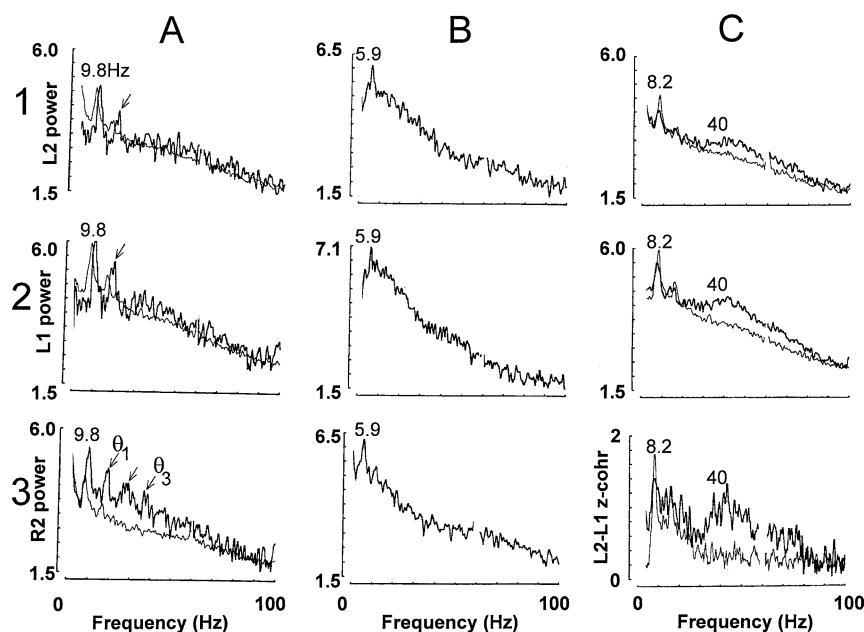


FIG. 5. Theta frequency during and gamma activity after a hippocampal-onset afterdischarge (AD) induced by i.c.v. CGP35348, as shown by EEG spectral analysis. EEGs were derived from the hippocampal-onset AD shown in Fig. 2; AD occurred at 31 min after injection of CGP35348 in rat S08. **A:** Power spectra for period "b" indicated in Fig. 2A (*dark traces*) at 1) L2, 2) L1, and 3) R2, overlaid with spectra during walking before CGP35348 (*light traces*). Note the 9.8 Hz theta peak (fundamental) with theta harmonics (*arrows*), in particular at electrode R2 (three harmonics clearly seen). θ_1 and θ_3 indicates first and third theta harmonic, respectively. **B:** Power spectra displayed as in part A, analyzed for a 10.2-s ictal period starting with period "d" in Fig. 2A, showing a mean peak frequency at 5.9 Hz for all electrodes. **C:** Power spectra at 13 min after the AD (*dark traces*) at C1) L1 and C2) L2. Note that part C3 is now the z-transform coherence spectrum (signals at L1 and L2). The coherence was high at theta (8.2 Hz) and gamma (peak, 40 Hz) frequencies. Light traces are spectra for the respective electrode during baseline walking. Degrees of freedom (df) of dark traces are 22 (**A**), 44 (**B**), and 88 (**C**); df for underlying light trace, 132. Peaks at 60 Hz (line power) were removed. Power peak of 4.8 log units is equivalent to a sine wave EEG signal of 0.5 mV peak-to-peak, and 6.8 log units = 5 mV EEG.

than at the hippocampal electrode L1 (see electrode location in Fig. 2 inset). The change from EEG spikes to an AD was characterized by an increase in the discharge frequency to >1 Hz. The maximal AD amplitude recorded at the deep layers of the neocortex was ~3 mV. Hippocampal EEG remained unchanged during the neocortical AD, as was shown in the polygraph recording (Fig. 3A) and confirmed by power spectral analysis (Fig. 6A2). The neocortical AD was shown as a power peak at 1.7 Hz at the neocortical electrode (Fig. 6A1). No postictal depression of hippocampal or neocortical EEG was found (not shown) if the AD did not spread into the hippocampus. Some neocortical-onset ADs did subsequently spread into the hippocampus and induced high-amplitude (>5 mV) discharges at hippocampal electrodes (not shown).

Forelimb clonus, body jerks, and generalized motor convulsions often accompanied the neocortical AD. In some rats, neocortical EEG spikes may be accompanied by rhythmic (<1 Hz) jerks of the hindlimb, contralateral to the site of CGP35348 injection. The contralateral limb jerks were not considered a behavioral seizure, and they were likely induced by diffusion of CGP35348 along the shaft of the cannula into the parietal and sensorimotor cortex.

Repeated afterdischarges induced by high-dose i.c.v. CGP35348

Repeated ADs may be induced by a single dose of i.c.v. CGP35348, more often at doses >110 μg i.c.v. (see Table 1). In 19 experiments in which a second AD was observed after CGP35348 injection, the duration of the second AD was found to be significantly longer than that of the first AD ($p < 0.05$, paired Wilcoxon). The duration of behavioral seizure also increased progressively with AD duration. However, only a trend ($p = 0.11$, paired Wilcoxon) was noted in that the seizure stage increased with the second as compared with the first AD. In the example shown, the rat first had a neocortical-onset AD at 16 min after CGP35348 injection (see Fig. 3A), before a hippocampal-onset AD at 31 min (Fig. 2A), and yet another hippocampal-onset AD at 46 min after injection (Fig. 3B). The last hippocampal AD was longer in duration than each of two earlier ADs. The duration of the period with bilateral forelimb clonus increased with the prolongation of AD duration (Fig. 3B). The second hippocampal AD was preceded by abnormal theta-frequency waves and ended with a rebound AD (Fig. 3B).

High doses of CGP35348 ($\geq 220 \mu\text{g}$, i.c.v.) typically evoked severe motor convulsions (Table 1). In almost all animals given 330 μg i.c.v. CGP35348, multiple

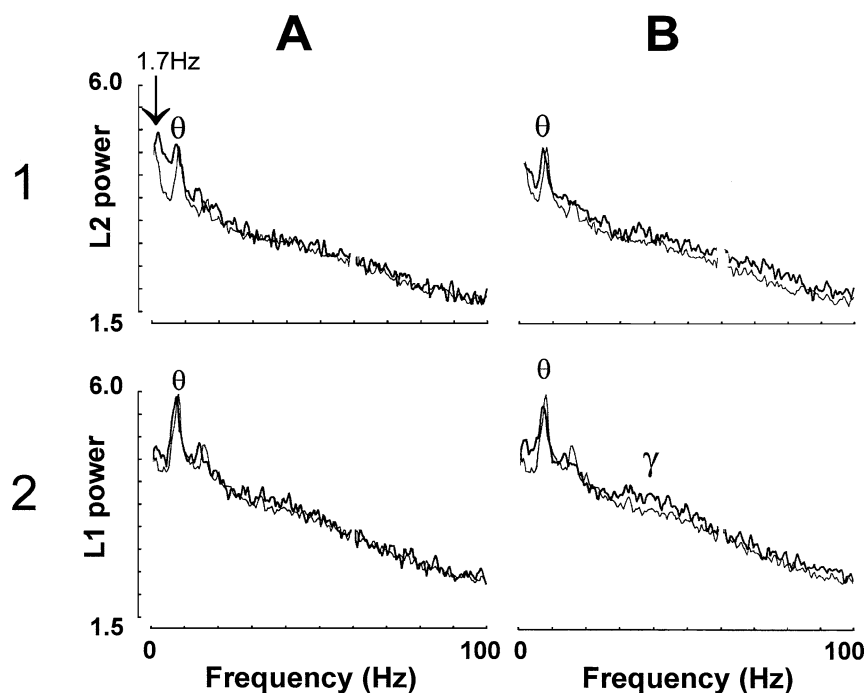


FIG. 6. Delta frequency during and little gamma-frequency change after a neocortical-onset afterdischarge (AD) induced by i.c.v. CGP35348. EEGs for the neocortical-onset AD are shown in Fig. 3A for rat S08. **A:** Power spectra of the EEG at electrodes L2 and L1 during walking before CGP35348 (*light traces*), overlaid with spectra during the first 10.2 s of the neocortical AD (*dark traces*) shown in Fig. 3A. The EEGs at L1 and L2 remained unchanged except for an additional 1.7-Hz low-frequency peak (main frequency of neocortical AD) at L2 (*arrow*). θ indicates theta power peak. **B:** Power spectra 13 min after the neocortical AD (*dark traces*), overlaid with baseline EEG before CGP35348 (*light traces*), showing only a small increase in gamma (γ) at ~ 40 Hz in the postictal EEG. *df*, >88 for all spectra.

running/jumping seizures associated with generalized ADs were observed.

Hippocampal gamma activity induced by GABA_B-receptor blockade and afterdischarge

Hippocampal gamma power showed no consistent change after i.c.v. CGP35348 injections if ADs were not evoked ($N > 8$ rats). However, if the EEGs were analyzed within 5 min before the onset of a hippocampal AD induced by CGP35348, a small increase in hippocampal gamma power at 30–60 Hz was detected (not shown). This increase in gamma activity was found during either walking or immobility of the rat. The increase of the peak gamma power (at 30–40 Hz) at the stratum radiatum electrode, immediately (<5 min) before the AD, was 0.28 ± 0.05 log units ($n = 6$ rats).

A large increase of hippocampal gamma activity was found after a hippocampal AD induced by i.c.v. CGP35348. Up to 30 min after a hippocampal AD, hippocampal gamma activity in the 25- to 80-Hz band was increased (Fig. 5C). At 8–15 min after the AD, the increase in gamma peak power (near 40 Hz) at the stratum radiatum electrode was 0.55 ± 0.07 log units ($n = 7$ rats), as compared with baseline gamma before injection. Electrodes across the CA1 cell layer showed an $\sim 180^\circ$ reversal in the polarity of gamma waves (not shown) and an increased coherence at the gamma frequency (Fig. 5C3). The increase in hippocampal gamma activity was independent of the

behavior of the rat, and it occurred consistently only after a hippocampal AD but not after a neocortical AD that did not invade the hippocampus. In the example shown, a small increase in gamma waves was shown at 13 min after the neocortical AD (Fig. 6B2).

Excitatory changes in the hippocampus before and after an afterdischarge

The excitability of the hippocampus was studied before and after CGP35348 injection, by using paired-pulse responses to apical dendritic stimulation of CA1. In seven experiments with five rats, CGP35348 (56–110 μg , i.c.v.) injection had no consistent effect on the first-pulse population spike or pEPSP, although the population spike was slightly increased after CGP35348 in the example shown (Fig. 7B). During baseline before drug, PPD of the population spikes and pEPSPs was apparent, as shown by PPD at 30-ms IPI in Fig. 7B. CGP35348 further increased the PPD at IPI <100 ms, before the occurrence of an AD (Fig. 7B). In each of five rats, the injection of CGP35348 (56 μg , i.c.v.) decreased the ratio of the pEPSP peaks (E2:E1) at 100-ms IPI from 1.10 ± 0.05 to 0.84 ± 0.04 ($p < 0.05$, paired Wilcoxon). A decrease in pEPSP peak ratio indicates an increase in PPD.

Excitability changes in CA1 also were monitored around the onset of the AD ($*$ in Fig. 7A). No abrupt change of evoked responses was detected preceding the AD induced by i.c.v. CGP35348 (five rats). In two rats,

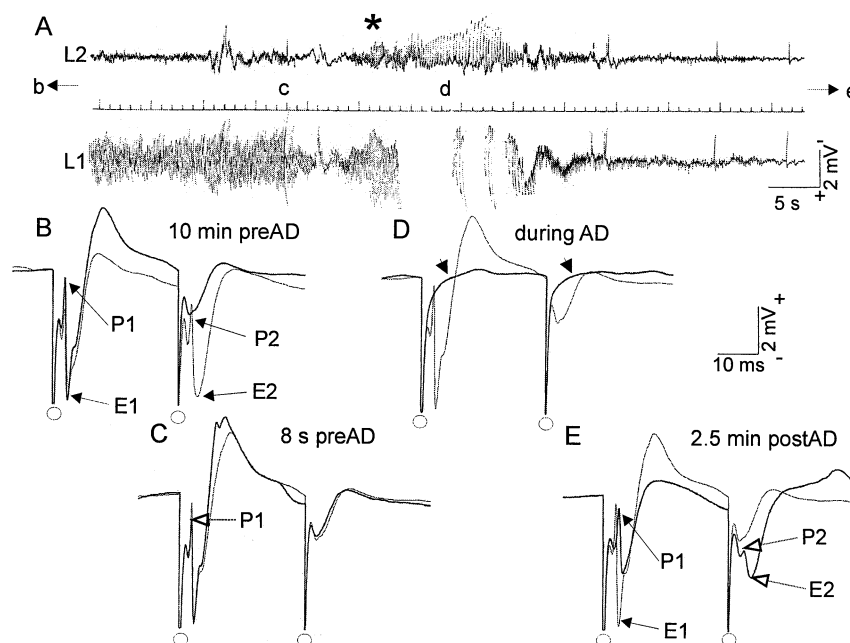


FIG. 7. Hippocampal paired-pulse depression was increased by CGP35348 i.c.v. and decreased after but not before a hippocampal afterdischarge (AD). **A:** Hippocampal AD induced by CGP35348 (56 μg , i.c.v.) recorded at two electrodes across the CA1 cell layer (**top**, electrode L2 at the alveus of CA1; **bottom**, electrode L1 at proximal stratum radiatum of CA1). The primary AD (starting at * with theta-frequency discharges), induced ~ 20 min after injection, was ~ 22 s long and was followed by a rebound AD (not shown). **B–E:** Paired-pulse responses recorded at the times “b” to “e” labeled in part **A**. Paired pulses at 30-ms interpulse interval were recorded at L1, after stimulation of stratum radiatum of CA1 ~ 2 mm posterior to L1 (stimulus intensity, 600 μA , 0.1-ms-duration pulses). **B:** Average responses (four sweeps were averaged) at 10 min after CGP35348 (**dark trace**) overlaid with average baseline response before CGP35348 (**light trace**). P1 (first pulse population spike) and population excitatory postsynaptic potential (pEPSP) after the first pulse (E1) was about the same, whereas population spike (P2) and pEPSP (E2) after the second pulse were depressed after CGP35348. **C:** Single-sweep response < 8 s before the onset of the AD (**dark trace**), at point “c” in part **A**, showing slight decrease of P1 (**open arrow**) as compared with the overlaid response 10 min before the AD (**light trace**). **D:** Same as **C** except **dark trace** is single-sweep response during AD, at point d in part **A**; **short arrows** indicate a lack of response, with only shock artifacts remaining. **E:** Same as **C** except **dark trace** is single-sweep response at 2.5 min after the AD, showing postictal depression of the first pulse population response P1 and E1 (**solid arrows**), but facilitation of P2 and E2 (**open arrows**). Rat R813.

evoked responses were recorded immediately (< 30 s) before the onset of the AD. A small decrease in population spike was seen immediately before the AD (arrow with open head, Fig. 7C). During the AD, synaptic response was abolished (short arrows, Fig. 7D). For > 10 min after the AD, the first pulse evoked a smaller population spike (P1) that occurred at a longer latency and rising from a smaller pEPSP (E1), as compared with before drug (Fig. 7E). The smaller E1 and P1 were characteristic of postictal depression, which was also accompanied by EEG depression (not shown). During postictal depression, however, the second-pulse response (population spike P2 or pEPSP E2) was increased, or PPD was partially blocked (Fig. 7E).

Afterdischarges/seizures induced by i.c.v. CGP55845A and CGP55699A

CGP55845A was relatively ineffective in inducing ADs or behavioral seizures. Only two of 13 injections with a dose of ≥ 0.84 μg i.c.v. CGP55845A resulted in a hippocampal AD (Table 2). The rare ADs in two rats consisted of 3- to 4-Hz paroxysmal activity, with no rebound AD or postictal depression, different from the typical hippocam-

pal AD described earlier. In two other experiments, abnormal behaviors consisted of leg jerks and facial clonus, respectively, with no concomitant change in hippocampal EEG. In rats that showed no seizure after CGP55845A, CGP35348 injection (28–110 μg , i.c.v.) was confirmed to induce ADs and behavioral seizures, just as in other rats given CGP35348.

TABLE 2. CGP55845A, i.c.v., induced few afterdischarges (ADs)

Dose of CGP 55845A (μg)	0.21	0.84	3.37	6.59	21.73
Estimated concentration (μM , i.c.v.)	0.32	1.28	5.12	10	33 ^b
Number of rats	2	6	3	1	3
Number showing AD in 1h	0	1	0	0	1
Percentage showing AD in 1h	0	17%	0	0	33%
Latency of AD onset (min) ^a		40			14
Duration of first AD (s) ^a		123			53
Mean behavioral seizure stage ^b		4			3

Except for the highest dose used, animals that had more than three injections and two or more afterdischarges (ADs) in previous injections were not included.

^aLatency and duration measures are of the single animal that had ADs.

^bSeizure stage according to classification of Racine (1972).

By contrast, CGP56999A (0.48 to 0.96 μg , i.c.v.) was effective in inducing hippocampal AD and behavioral seizures. Two of four rats given a dose of 0.48 μg , i.c.v., showed a hippocampal AD at 16 and 70 min, respectively. All three rats given 0.96 μg , i.c.v., showed repeated seizures, with more than four ADs in the hippocampus in 2 h.

In five experiments with four freely moving rats, PPD of the evoked responses in CA1 was studied after i.c.v. CGP55845A (0.84–3.36 μg) injections. At 100-ms IPI, the paired-pulse ratio of the pEPSP peaks was 1.30 ± 0.03 ($n = 5$) during baseline before drug injection, and 1.10 ± 0.16 after CGP55845A, not significantly different from baseline ($p = 0.14$, paired Wilcoxon).

CGP35348 and CGP55845A were further tested for their antagonism of the effect of GABA_B-receptor agonist baclofen on the hippocampus (Methods). Evoked potentials were recorded at stratum radiatum of CA1 after high-intensity stimulation ($>200 \mu\text{A}$, 0.1-ms pulse duration) of CA3 in urethane-anesthetized rats (Fig. 8). Injection of \pm baclofen (10 nmole, i.c.v.) induced a depression of the first-pulse pEPSP (E1 at solid arrow in Fig. 8A) and an increase in the second-pulse pEPSP and population spike (open arrow in Fig. 8A). Thus the paired-pulse pEPSP ratio was increased by i.c.v. baclofen (Table 3). When rats were

pretreated with CGP35348 (93 μg or 400 nmole, i.c.v.), the effect of baclofen on the evoked responses was almost completely abolished (Fig. 8B), as confirmed by the lack of change of pEPSP measures after the combination of CGP35348 and baclofen, as compared with the predrug baseline (Table 3). Pretreatment with CGP55845A (1.28 to 2.56 μg ; or 2.9 to 5.8 nmole), however, did not block the effects of baclofen. Baclofen's effect in decreasing E1 or increasing paired-pulse EPSPs (E2/E1) was not different with or without CGP55845A (Table 3).

DISCUSSION

CGP35348-induced hippocampal ADs

The high-amplitude discharges of >5 mV seen at hippocampal electrodes after i.c.v. CGP35348 injection were clearly generated in the hippocampus. Typically, the high-amplitude ADs showed reversed polarity across the electrodes that straddled the CA1 cell layer and a long AD (of >20 s duration) induced postictal depression of the hippocampal EEG (Fig. 1C) and the hippocampal evoked potentials (Fig. 7D). Recordings in the parietal cortex, amygdala, and entorhinal cortex did not reveal paroxysmal activity that preceded the high-amplitude ADs in the hippocampus. However, it should be noted that the exact location where the AD actually started is difficult to ascertain with a limited number of electrodes.

Strikingly similar features were found between the ADs evoked by low doses of i.c.v. CGP35348 and the ADs evoked by electrical stimulation of the hippocampus (17). The sequence of primary followed by rebound discharges with wet-dog shakes and postictal EEG depression was the same in electrically evoked and CGP35348-induced hippocampal ADs. Both electrically and CGP35348-induced ADs likely involve most of the neurons in CA1, thus giving high-amplitude (>5 mV) paroxysmal discharges.

A robust increase of hippocampal gamma waves was found 5–30 min after a hippocampal AD induced by CGP35348 (Fig. 5C). The amplitude, frequency, location, and duration of the hippocampal gamma waves after the CGP35348-induced AD were in all aspects similar to the gamma waves after an electrically evoked AD (17,22). In total, these observations suggest that hippocampal gamma waves increased after a hippocampal AD, irrespective whether the AD was induced electrically or chemically.

CGP35348 i.c.v. also was found to increase slightly the hippocampal gamma activity immediately before a hippocampal AD (Results). Gamma activity is likely generated by local neural circuits that involve GABAergic neurons (23–26). An increase in GABA_A receptor-mediated inhibition was inferred after GABA_B-receptor blockade, manifested as an increase in PPD at <100 ms IPI (discussed earlier). We suggest that this enhancement of GABA_A-receptor function is sufficient to explain the increase in hippocampal gamma activity at 30–60 Hz,

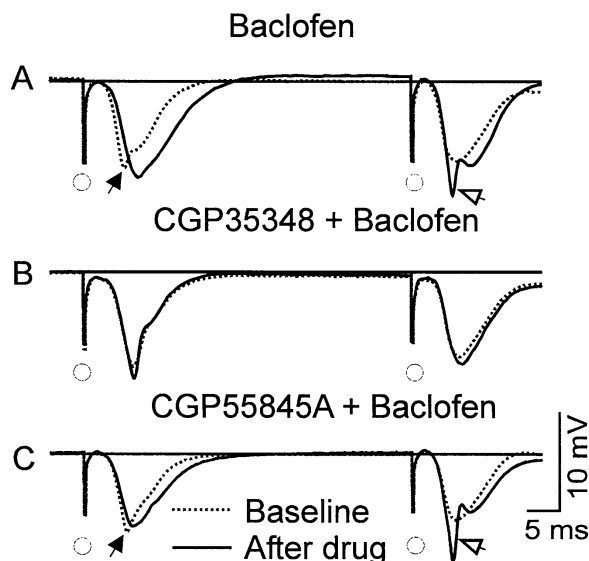


FIG. 8. The effect of baclofen on hippocampal average evoked potentials (AEPs) was blocked by i.c.v. CGP35348 but not i.c.v. CGP55845A. AEPs were recorded at stratum radiatum of CA1, after high-intensity (200–350 μA) paired-pulse stimulation of CA3, shown for 50-ms interpulse interval. Baseline refers to the AEP recorded before any drug; “After drug” refers to AEP recorded after all drugs (last one being baclofen). Baclofen (10 nmole i.c.v.) alone decreased the first-pulse EPSP (E1, arrow) and increased the second-pulse EPSP (E2) and population spike (open arrow). **B:** Baclofen's effect was blocked by injection of CGP35348 (i.c.v. 93 μg or 400 nmole) \sim 30 min before baclofen. **C:** Baclofen's effect was not blocked after prior injection of CGP55845A (i.c.v. 2.56 μg or 5.8 nmole); arrows indicate events as in **A**. Open circles indicate shock artifacts.

TABLE 3. The effect of \pm baclofen (10 nmole) on population excitatory postsynaptic potentials (pEPSPs)

	No. of rats	First-pulse pEPSP (E1)	Second-pulse pEPSP (E2)	E2:E1
Baclofen alone	6	67 \pm 6%	160 \pm 23%	245 \pm 37%
CGP35348 + baclofen	3	102 \pm 2% ^a	104 \pm 11%	102 \pm 11% ^a
CGP55845A + baclofen	3	91 \pm 14%	155 \pm 17%	176 \pm 24%

The effect was blocked by CGP35348 (400 nmole or 93 μ g i.c.v.) but not by CGP55845A (2.9–5.8 nmole or 1.28–2.56 μ g, i.c.v.). Percentage change of pEPSP measures from the baseline (before drug) is shown. pEPSP slope was analyzed by the rising slope of the maximal current sink at CA1 stratum radiatum (Methods).

^ap < 0.05, Wilcoxon, significantly different from baclofen-alone group. Values not labeled are not significantly different from those of the baclofen-alone group.

before an AD. An increase in hippocampal gamma (and beta) activity has been reported after drugs that increased GABA_A-receptor currents (27). Richards et al. (28) found an increase in power at 21.5–30 Hz (beta frequency) in the neocortex of rats after CGP56999 injection; gamma EEG was not studied.

Theta-frequency afterdischarges

CGP35348-induced hippocampal ADs started at 5–9 Hz, which is higher than the onset frequency of electrically evoked ADs. The electrically evoked ADs in dorsal hippocampal CA1 started at <4 Hz (Fig. 4B; see also ref. 29), although hippocampal ADs evoked by electrical or chemical (*N*-methyl-D-aspartate) stimulation of the ventral subiculum started with 4–7 Hz (30). Mechanisms underlying the ictal discharges are not fully understood. Computer simulation suggested that the frequency of in vitro ADs may be controlled by recurrent excitation, inhibition, and voltage-dependent events (31). The intrinsic membrane potential oscillations of hippocampal CA3 and CA1 neurons (32–35) also may contribute to the theta-frequency AD.

GABA_B-receptor antagonist CGP35348, i.c.v., increased the average initial frequency of the electrically evoked ADs in the hippocampus from 3.6 to 5.3 Hz (Results). This may also explain why the onset frequency of a CGP35348-induced AD was relatively high, with a 6.4-Hz mean frequency. CGP35348 facilitated paired-pulse CA1 response to CA3 stimulation mostly at 160–400 ms IPI, equivalent to 2.5–6 Hz (Peloquin, Canning, and Leung, unpublished data). A single discharge in the AD will be followed by voltage- and Ca²⁺-activated K⁺-mediated hyperpolarization as well as a GABA_B receptor-mediated inhibition; thus blocking GABA_B receptor-mediated inhibition would reduce the interval between discharges.

We found that CGP35348 induced a 9- to 10-Hz theta-frequency EEG in the hippocampus immediately before a hippocampal AD (Figs. 2A and 5B). The abnormal theta may contribute to but was not essential for AD generation, because some hippocampal ADs occurred without the abnormal theta episode (Fig. 1A). The coherence and phase of the 9- to 10-Hz EEG were similar to the normal hippocampal theta of lower peak frequency (<9 Hz). An increase in theta harmonics (sharper waves) with in-

creasing theta frequency was reported (36). We also observed that CGP35348 could induce theta waves of 5–8 Hz when the rat was completely immobile (not shown), perhaps consistent with the effect of CGP35348 in increasing carbachol-induced hippocampal theta oscillations in vitro (33,37). In a normal rat, theta waves of >9 Hz would be accompanied by vigorous movements, such as those during initiation of running or ballistic jumping (38,39), but only for a duration of <1 s. However, the 9- to 10-Hz waves reported here after CGP35348 were accompanied by apparently normal locomotion and lasted for >10 s.

Many rats jumped vertically during the theta-frequency ADs. A brief series of jumps may not be associated with other motor convulsions. We suggest that an increased response to sensorimotor stimulation induced the reflexive, stereotypic jumps.

Motor seizure and kindling with GABA_B-receptor blockade

The first hippocampal AD induced by CGP35348 was often accompanied by motor convulsive behaviors such as bilateral forelimb, facial, and body clonus (Fig. 2). The convulsions were bilateral, and a progression from stage 3 to stage 5 seizures is characteristic of hippocampal and other limbic ADs. However, in normal rats, electrical kindling of the dorsal and ventral hippocampus required a mean of 51 and 27 ADs, respectively, to reach stage 5 seizure (40) and at least half these numbers to reach stage 3 seizure. In addition, neocortical ADs induced by i.c.v. CGP35348 often drive a hippocampal AD, whereas without GABA_B-receptor blockade, more than 10 cingulate and even more neocortical ADs were required to drive a hippocampal AD (41).

We suggest that GABA_B-receptor blockade facilitates both the initiation and the spread of a seizure, such that generalized convulsions may be driven by a hippocampal AD. We showed that the AD threshold in the hippocampus was lowered by GABA_B-receptor blockade (Results), and the same may apply to other brain areas. Neocortical EEG spikes and isolated limb clonus indicate the disinhibition in the neocortex. Frequency potentiation at 2.5–6 Hz was increased after i.c.v. CGP35348 (see earlier) and 2.5- to 6-Hz activity propagates optimally through the entorhinal-hippocampal circuit and other multisynaptic

circuits (42,43). Thus the spread of an AD will be facilitated with GABA_B-receptor blockade, perhaps explaining why amygdala kindling was accelerated with GABA_B-receptor blockade (44).

High doses of CGP35348 (220–330 μg , i.c.v.) often induced generalized seizures. After 330 μg i.c.v. CGP35348, severe clonic–tonic seizures with jumping and running started without apparent provocation. The origin of these rapidly generalized seizures was difficult to determine, because ADs appeared simultaneously in most implanted electrodes. It is possible that massive ADs in the hippocampus may spread quickly to other structures, or the seizures were generalized from the onset. Some of the severe running and jumping may be a result of brain-stem seizures (45,46).

More than one AD may be induced by a single injection of i.c.v. CGP35348 or CGP56999A. A single dose of a GABA_B-receptor antagonist induced ADs of increasing duration, with a statistical trend of increasing seizure severity. The results suggest that kindling occurred in the hippocampus (47), although pharmacokinetics (prolonged action of a single dose of CGP35348) also could explain the results.

Hippocampal excitability after GABA_B-receptor blockade

We reported that PPD in CA1, at 30- to 100-ms IPIs, was increased by CGP35348 (56 μg , i.c.v.) in the freely moving rat. This extends the result that PPD in the dentate gyrus increased after a high dose of CGP35348 (> 110 μg , i.c.v.) in urethane-anesthetized rats (48,49).

PPD of the population spike or pEPSP at <100-ms IPI is likely mediated by an increase in the postsynaptic GABA_A-receptor-mediated inhibition evoked by the first pulse (49,50). Single-pulse GABA_A-IPSP was not changed by CGP35348 in hippocampal slices in vitro (14,50). However, GABA_B autoreceptors are presumably tonically active in the hippocampus in vivo (Peloquin and Leung, unpublished data), and their blockade would enhance GABA release by a single afferent stimulus pulse. Blockade of GABA_B postsynaptic receptors on GABAergic interneurons (51) also may enhance interneuronal firing that will increase the evoked postsynaptic inhibition on principal cells.

Little change in single-pulse or paired-pulse Schaffer collateral-mediated population spikes or pEPSPs was found in CA1 before the AD. Similarly, Buckmaster et al. (52,53) did not find a change in perforant-path evoked response in the dentate gyrus preceding a spontaneous seizure in gerbils. In addition, Buckmaster et al. (52) reported a decrease in PPD after a seizure, similar to our result. However, when paired pulses of 20-ms IPI were delivered at 5 Hz to the perforant path to evoke an AD, a loss of PPD in the dentate gyrus was shown to precede the electrically evoked AD by <2 s (54). For technical

reasons (we stimulated every 9 s), we were unable to test CA1 excitability at <5 s from the onset of a CGP35348-induced AD. Thus we could not exclude the possibility that a sudden and brief (<5 s) excitability change in CA1 precedes a CGP35348-induced AD.

Dose response of various GABA_B-receptor antagonists

CGP55845A, although given in estimated effective concentrations (1–5 μM , i.c.v.), had little effect on hippocampal PPD or seizures. Similarly, i.c.v. CGP35348 but not CGP55845A blocked the effects of i.c.v. baclofen on hippocampal CA1 evoked potentials. We suggest that i.c.v. CGP55845A penetrates the ventricle–brain barrier only with difficulty, as compared with CGP35348 or CGP56999A, but we are not aware of any supporting evidence, and i.p. CGP55845A was presumably effective in the brain (55).

The relatively low dose of CGP35348 (56 μg estimated to give a concentration of 160 μM) in the ventricle suggests that postsynaptic GABA_B-receptor blockade was sufficient to elicit hippocampal ADs. CGP35348 concentration of ~160 μM in vitro blocked postsynaptic but not presynaptic GABA_B receptors in hippocampal CA1 (14,15). However, the exact concentration of CGP35348 in neural tissue in vivo has not been determined, and questions have been raised whether the in vivo effects of CGP35348 are the same as those in vitro (48,49). In fact, 56 μg i.c.v. CGP35348 was effective in attenuating theta-frequency primed burst long-term potentiation (LTP) in CA1 of freely moving rats (Leung and Shen, unpublished data), whereas the estimated equivalent of 160 μM did not block LTP in vitro (14).

Summary

Based on electrophysiologic and behavioral observations, we showed that partial seizures were induced in the hippocampus by GABA_B-receptor blockade with CGP35348 and CGP56999A but not with CGP55845A. Hippocampal ADs induced by GABA_B-receptor blockade started with theta-frequency discharges, which may be accompanied by jumping and stage 3/4 seizures. We suggest that GABA_B-receptor blockade induced seizures by lowering the AD threshold, increasing AD-onset frequency, and facilitating the spread of ADs.

Acknowledgment: This work was supported by CIHR grants MOP-64433 and 36421 and an NSERC grant. We thank the Alzheimer Society of Canada for providing a Doctoral Training Award to K.J.C. The experiments on urethane-anesthetized rats were performed by Pascal Peloquin. We thank Dr. W. Froestl for the GABA_B-receptor antagonists, and Dr. Froestl and Dr. J. Ma, for comments.

REFERENCES

1. Krnjevic K. Significance of GABA in brain function. In: Tunnicliff G, Raess BU, eds. *GABA mechanisms in epilepsy*. New York: Wiley, 1991:47–87.

2. Engel JJ. Excitation and inhibition in epilepsy. *Can J Neurol Sci* 1996;23:167-74.
3. Snead OC III. Basic mechanisms of generalized absence seizures. *Ann Neurol* 1995;37:146-57.
4. Bowery NG, Bettler B, Froestl W, et al. International Union of Pharmacology. XXXIII: Mammalian gamma-aminobutyric acid(B) receptors: structure and function. *Pharmacol Rev* 2002;54:247-64.
5. Vergnes M, Boehrer A, Simler S, et al. Opposite effects of GABA_B receptor antagonists on absences and convulsive seizures. *Eur J Pharmacol* 1997;332:245-55.
6. Badran S, Schmutz M, Olpe HR. Comparative in vivo and in vitro studies with the potent GABA_B receptor antagonist, CGP 56999A. *Eur J Pharmacol* 1997;333:135-42.
7. Vergnes M, Boehrer A, Reibel S, et al. Selective susceptibility to inhibitors of GABA synthesis and antagonists of GABA_A receptor in rats with genetic absence epilepsy. *Exp Neurol* 2000;161:714-23.
8. Malouf AT, Robbins CA, Schwartzkroin PA. Baclofen inhibition of the slow inhibitory postsynaptic potential in hippocampal slice cultures: a possible role for the GABA_B-mediated inhibitory postsynaptic potential. *Neuroscience* 1990;35:53-61.
9. Uusisaari M, Smirnov S, Voipio J, et al. Spontaneous epileptiform activity mediated by GABA_A receptors and gap junctions in the rat hippocampal slice following long-term exposure to GABA_B antagonists. *Neuropharmacology* 2002;43:563-72.
10. Gambardella A, Manna I, Labate A, et al. GABA(B) receptor 1 polymorphism (G1465A) is associated with temporal lobe epilepsy. *Neurology* 2003;60:560-3.
11. Prosser HM, Gill CH, Hirst WD, et al. Epileptogenesis and enhanced prepulse inhibition in GABA(B1)-deficient mice. *Mol Cell Neurosci* 2001;17:1059-70.
12. Schuler V, Luscher C, Blanchet C, et al. Epilepsy, hyperalgesia, impaired memory, and loss of pre- and postsynaptic GABA(B) responses in mice lacking GABA(B1). *Neuron* 2001;31:47-58.
13. Paxinos G, Watson C. *The rat brain in stereotaxic coordinates*. San Diego: Academic Press, 1986.
14. Davies CH, Starkey SJ, Pozza MF, et al. GABA autoreceptors regulate the induction of LTP. *Nature* 1991;349:609-11.
15. Karlsson G, Kolb C, Hausdorf A, et al. GABA_B receptors in various in vitro and in vivo models of epilepsy: a study with the GABA_B receptor blocker CGP 35348. *Neuroscience* 1992;47:63-8.
16. Davies CH, Pozza MF, Collingridge GL. CGP 55845A: a potent antagonist of GABA_B receptors in the CA1 region of rat hippocampus. *Neuropharmacology* 1993;32:1071-3.
17. Leung LS. Hippocampal electrical activity following local tetanization, I: afterdischarges. *Brain Res* 1987;419:173-87.
18. Leung LS, Wu C, Wu K, Shen B, et al. Long-lasting behavioral and electrophysiological effects induced by partial hippocampal kindling. In: Corcoran ME, Moshe S, eds. *Kindling 5*. New York: Plenum Press, 1998:395-408.
19. Racine RJ. Modification of seizure activity by electrical stimulation, II: motor seizure. *Electroencephalogr Clin Neurophysiol* 1972;32:281-94.
20. Leung LS, Lopes da Silva FH, Wadman WJ. Spectral characteristics of the hippocampal EEG in the freely moving rat. *Electroencephalogr Clin Neurophysiol* 1982;54:203-19.
21. Kloosterman F, Peloquin P, Leung LS. Apical and basal orthodromic population spikes in hippocampal CA1 in vivo show different origins and patterns of propagation. *J Neurophysiol* 2001;86:2435-44.
22. Ma J, Leung LS. Medial septum mediates the increase in postictal behaviors and hippocampal gamma waves after an electrically induced seizure. *Brain Res* 1999;833:51-7.
23. Leung LS. Nonlinear feedback model of neuronal populations in hippocampal CA1 region. *J Neurophysiol* 1982;47:845-68.
24. Jefferys JGR, Traub RD, Whittington MA. Neuronal networks for induced "40 Hz" rhythms. *Trends Neurosci* 1996;19:202-8.
25. Traub RD, Jefferys JG, Whittington MA. Simulation of gamma rhythms in networks of interneurons and pyramidal cells. *J Comput Neurosci* 1997;4:141-50.
26. Leung LS. Generation of theta and gamma rhythms in the hippocampus. *Neurosci Biobehav Rev* 1998;22:275-90.
27. Leung LS. Spectral analysis of hippocampal EEG in the freely moving rat: effects of centrally active drugs and relations to evoked potentials. *Electroencephalogr Clin Neurophysiol* 1985;60:65-77.
28. Richards DA, Morrone LA, Bowery NG. Hippocampal extracellular amino acids and EEG spectral analysis in a genetic rat model of absence epilepsy. *Neuropharmacology* 2000;39:2433-41.
29. Bragin A, Csicsvari J, Penttonen M, et al. Epileptic afterdischarge in the hippocampal-entorhinal system: current source density and unit studies. *Neuroscience* 1997;76:1187-203.
30. Ma J, Brudzynski SM, Leung LS. A role of subicular and hippocampal afterdischarges in initiation of locomotor activity in rats. *Brain Res* 1998;793:112-8.
31. Traub RD, Borck C, Colling SB, et al. On the structure of ictal events in vitro. *Epilepsia* 1996;37:879-91.
32. Konopacki J, MacIver MB, Bland BH, et al. Carbachol-induced EEG "theta" activity in hippocampal brain slices. *Brain Res* 1987;405:196-8.
33. Konopacki J, Golebiewski H, Eckersdorf B, et al. Theta-like activity in hippocampal formation slices: the effect of strong disinhibition of GABA_A and GABA_B receptors. *Brain Res* 1997;775:91-8.
34. Leung LS, Yim CY. Intrinsic membrane potential oscillations in hippocampal neurons in vitro. *Brain Res* 1991;553:261-74.
35. Cobb SR, Buhl EH, Halasy K, et al. Synchronization of neuronal activity in hippocampus by individual GABAergic interneurons. *Nature* 1995;378:75-8.
36. Leung LS. Theta rhythm during REM sleep and waking: correlations between power, phase and frequency. *Electroencephalogr Clin Neurophysiol* 1984;58:553-64.
37. Scanziani M. GABA spillover activates postsynaptic GABA_B receptors to control rhythmic hippocampal activity. *Neuron* 2000;25:673-81.
38. Vanderwolf CH. Hippocampal electrical activity and voluntary movement in the rat. *Electroencephalogr Clin Neurophysiol* 1969;26:407-18.
39. Whishaw IQ, Vanderwolf CH. Hippocampal EEG and behavior: changes in amplitude and frequency of RSA (theta rhythm) associated with spontaneous and learned movement patterns in rats and cats. *Behav Biol* 1973;8:461-84.
40. Racine R, Rose PA, Burnham WM. Afterdischarge thresholds and kindling rates in dorsal and ventral hippocampus and dentate gyrus. *Can J Neurol Sci* 1977;4:273-8.
41. Leung LS, Boon KA. Kindling in the posterior cingulate cortex: electrographic and behavioural characteristics. *Electroencephalogr Clin Neurophysiol* 1990;76:177-86.
42. Ziakopoulos Z, Brown MW, Bashir ZI. GABA_B receptors mediate frequency-dependent depression of excitatory potentials in rat perirhinal cortex in vitro. *Eur J Neurosci* 2000;12:803-9.
43. Yeckel MF, Berger TW. Spatial distribution of potentiated synapses in hippocampus: dependence on cellular mechanisms and network properties. *J Neurosci* 1998;18:438-50.
44. Karlsson G, Klebs K, Hafner T, et al. Blockade of GABA_B receptors accelerates amygdala kindling development. *Experientia* 1992;48:748-51.
45. Gale K. Subcortical structures and pathways involved in convulsive seizure generation. *J Clin Neurophysiol* 1992;9:264-77.
46. Browning R, Maggio R, Sahibzada N, et al. Role of brainstem structures in seizures initiated from the deep prepiriform cortex of rats. *Epilepsia* 1993;34:393-407.
47. Goddard GV, McIntyre DC, Leech CK. A permanent change in brain function resulting from daily electrical stimulation. *Exp Neurol* 1969;25:295-330.
48. Brucato FH, Morrisett RA, Wilson WA, et al. The GABA_B receptor antagonist, CGP-35348, inhibits paired-pulse disinhibition in the rat dentate gyrus in vivo. *Brain Res* 1992;588:150-3.
49. Canning KJ, Leung LS. Excitability of rat dentate gyrus granule cells in vivo is controlled by tonic and evoked GABA(B) receptor-mediated inhibition. *Brain Res* 2000;863:271-5.
50. Leung LS, Fu X. Factors affecting paired-pulse facilitation in hippocampal CA1 neurons in vitro. *Brain Res* 1994;650:75-84.
51. Forti M, Michelson HB. Synaptic connectivity of distinct hilar interneuron subpopulations. *J Neurophysiol* 1998;79:3229-37.

52. Buckmaster PS, Jongen-Relo AL, Davari SB, et al. Testing the disinhibition hypothesis of epileptogenesis in vivo and during spontaneous seizures. *J Neurosci* 2000;20:6232–40.
53. Buckmaster PS, Wong EH. Evoked responses of the dentate gyrus during seizures in developing gerbils with inherited epilepsy. *J Neurophysiol* 2002;88:783–93.
54. Tuff LP, Racine RJ, Adamec R. The effects of kindling on GABA-mediated inhibition in the dentate gyrus of the rat, I: Paired-pulse depression. *Brain Res* 1983;277:79–90.
55. Getova DP, Bowery NG. Effects of high-affinity GABAB receptor antagonists on active and passive avoidance responding in rodents with gamma-hydroxybutyrolactone-induced absence syndrome. *Psychopharmacology (Berl)* 2001;157:89–95.